Nanoporosity of an organo-clay shown by hyperpolarized xenon and 2D NMR spectroscopy†

Piero Sozzani,* Silvia Bracco, Angiolina Comotti, Michele Mauri, Roberto Simonutti and Patrizia Valsesia

Received (in Cambridge, UK) 13th February 2006, Accepted 21st February 2006
First published as an Advance Article on the web 6th March 2006
DOI: 10.1039/b602040b

Interlayer nanoporosity of hectorite pillared by tetraethylammonium ions is explored by hyperpolarized xenon NMR and relevant gases such as carbon dioxide revealing the adsorption capacity of the open galleries.

Nanoporous materials are attracting a great deal of scientific and technological interest for their ability to separate and store gas atoms and molecules. A material with small-sized pores is competitive with materials of large or giant pore-size not so much for its adsorption capacity but for the selectivity, specificity and sorption it shows at low pressure.[1] The nature of the constituent matter can range from fully inorganic[2] and metallo-organic[3] to organic materials.[4] Most structures present a framework of building blocks that form nanochannels or interconnected cages, but less commonly they are constituted by a skeleton of inorganic nanolayers.[5] A possible way to incorporate porosity in a nanolayered material is the intercalation, between the layers, of spacers such as inorganic ions and colloids or simply large organic ions.[6] Here we show, for the first time, the microporosity of an organohectorite by 2D advanced solid-state NMR techniques and its sorption properties with respect to xenon and gases important for energetic and environmental reasons such as methane and carbon dioxide. Rare spectroscopic observations were performed on the adsorbed gases. We applied laser enhanced hyperpolarized xenon NMR to demonstrate the nanoporosity of the material at high sensitivity and extremely low partial pressure of xenon.[7] The technique offers a great advantage over conventional Xe NMR spectroscopy, especially in the continuous flow set-up, demonstrating the accessibility of the cavities from the gas phase after short diffusion times. Tetraethylammonium hectorite (TEA-hectorite) was prepared in the presence of tetraethylammonium cations that counterbalance the negative charges of the inorganic layers (Fig. 1). Bulky cations are placed as pillars between the interlayers to keep them about 6 Å apart. It can be expected that the cations will not pack densely because of the charge repulsion and the stoichiometric balance that generates empty interpillar spaces. Until now this potential porosity has not been explored or characterized.

TEA-hectorite was prepared by hydrothermal synthesis with a formal stoichiometry $Ex_{0.66}(Mg_{5.34},Li_{0.66})Si_8O_{20}(OH,F)_4$,[8] where Ex is the exchangeable monocation TEA or Li^+. The content of TEA was determined to be 0.5 moles by thermogravimetric analysis and the peak due to the *d*(001) repeat period was observed at 14.7 Å by powder X-ray diffraction (Supporting Information). The presence of the organic cation in the interlamellar space, in close contact with the inorganic walls, was evidenced by the ^1H–^{29}Si 2D Heterocorrelated MAS NMR spectrum at 7.04 T, performed at high spinning speed (15 kHz) with Lee–Goldburg homonuclear decoupling that allows optimal resolution in the hydrogen domain.[9]

When the hydrogens in the ammonium ethyl moieties sit at short distances with respect to ^{29}Si, they can transfer magnetization to the observed nucleus, and a correlation signal is shown in the 2D ^1H–^{29}Si spectrum. Fig. 2a highlights the through-space interaction of the methylene and methyl hydrogens of TEA (δ_H = 3.0 and 0.5 ppm, respectively) with silicon Q^3 $Si(OSi)_3$ at δ_{Si} = −95.1 ppm in the hybrid material (the signal at δ_H = 0.5 ppm overlaps the silanol groups bonded to the Q^3 species). In support of the assignment of the TEA protons, the 2D ^1H–^{13}C Heterocorrelated Lee–Goldburg NMR spectrum (Fig. 2b) shows the correlation of TEA hydrogens covalently bonded to both methylene and methyl carbons at δ_C = 52.0 and 5.6 ppm, respectively. These experiments allowed us to detect, separately, carbon, silicon and hydrogen in magnetic communication one with the other and provide direct proof of the intimate relationships between the organic and inorganic components; they are one of the few examples of direct detection of hybrid interfaces by 2D NMR.[9] Considering the 9 Å thickness of the inorganic lamellae and the 6 Å diameter of the cations, the overall height of the layer

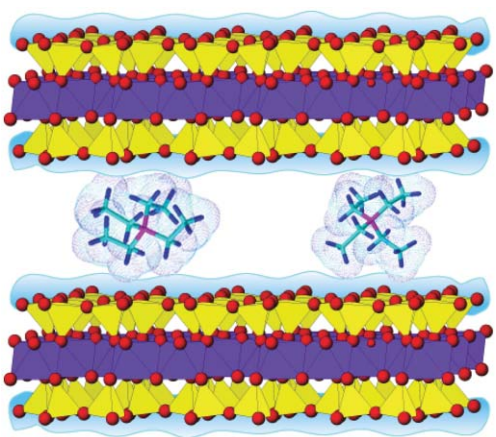

Fig. 1 Pillared structure of TEA-hectorite. It consists of inorganic pockets of two tetrahedral silicate layers (yellow) condensed to a central magnesium oxide octahedral layer (blue) intercalated by tetraethylammonium cations.

Department of Materials Science, University of Milano Bicocca, INSTM, Via R. Cozzi 53, Milan, Italy.
E-mail: piero.sozzani@mater.unimib.it; Fax: +39 02 6448 5140; Tel: +39 02 6448 5124

† Electronic supplementary information (ESI) available: Fig. S1. Powder X-ray diffraction of TEA-hectorite; Fig. S2. Pore distribution as obtained by the Horvath–Kavazoe method. See DOI: 10.1039/b602040b

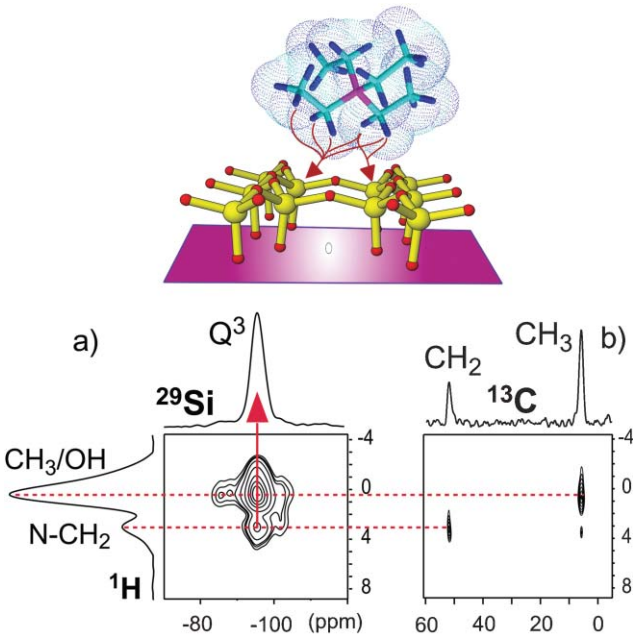

Fig. 2 Schematic representation of the intimate relationship between the tetraethylammonium cation and the silicate surface of the inorganic sheet (above) and 2D NMR spectroscopy: a) ^{1}H–^{29}Si Lee–Goldburg MAS NMR of the TEA-hectorite at a spinning speed of 15 kHz and a contact time of 8 ms; b) ^{1}H–^{13}C Lee–Goldburg MAS NMR of the TEA-hectorite with a contact time of 2 ms.

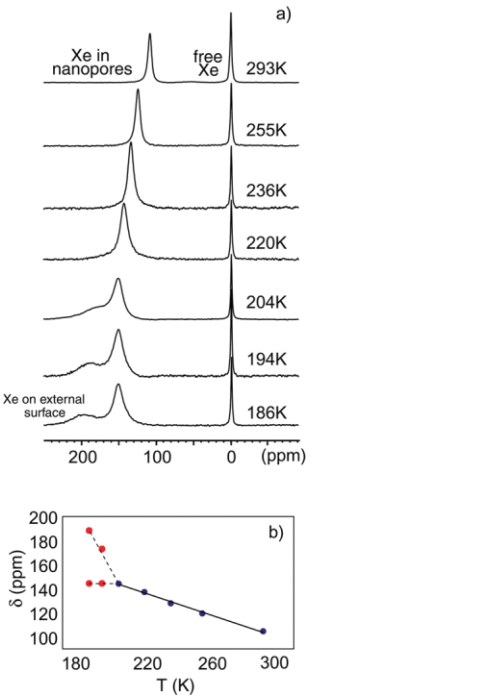

Fig. 3 a) Continuous Flow Hyperpolarized ^{129}Xe NMR spectra of xenon diffusing in the interpillar structure of TEA-hectorite at variable temperature. At low temperature an extra signal due to the xenon on the external surface is detected. b) Xe chemical shifts as a function of temperature.

is evaluated to be 15 Å, in agreement with the powder X-ray diffraction data.

The surface area, 330 $m^2\ g^{-1}$ determined by the BET method on N_2 adsorption data at 77 K, follows a type IV curve.[10] The Horvath–Kavazoe method and a slit-pore model revealed the micropore distribution of the material to be centered at 6 Å. A valuable probe gas for the exploration of nanocavities is xenon, which has a van der Waals radius of 2.2 Å and enters the interlayer pores easily, giving rise to a Xe NMR signal that is sensitive to the dimension of the confined spaces. Continuous Flow Laser-assisted Xenon NMR with its high sensitivity and low partial pressure is the method of choice for exploring small and large cavities.[7] The TEA-hectorite powder is placed in a homogeneous magnetic field through which there is a continuous flow of hyperpolarized Xe; after a few scans an intense resonance of xenon diffused inside the open cavities can be collected. At room temperature the signal at 105 ppm, downfield from the free-gas resonance, is indicative of the gas confined to the restricted spaces (Fig. 3a). Such a high value falls within the chemical shift range observed for microporous materials investigated at the limit of diluted xenon. In the case of our hyperpolarized xenon experiments the concentration is as low as 1.25% with a partial pressure of 9.5 torr. At the diluted limit the Xe-probe samples the interaction with the surrounding surface, with the advantage that the Xe–Xe interactions become negligible. Under these conditions the chemical shift δ_s due solely to interactions with the surfaces, depends on the mean free path l that defines the size of the explored micropores as $\delta_s = 243*2.054/(2.054 + l)$, according to a semiempirical model proposed by Fraissard.[11] Taking into account the xenon diameter, the pore size is evaluated as 7 Å. This is consistent with the interlamellar spacing generated by the pillars in the clay, as previously determined by 2D NMR experiments, and also indicates that the ammonium pillars are effective in restricting the *in-plane* movement of xenon within a space of about 7 Å. In addition, from the Xe NMR data and the stoichiometry we can evaluate the average microscopic space of the void explored by the xenon atoms; indeed this void is twice as large as the space occupied by a single ammonium pillar, indicating that a remarkable 70% of the interlamellar volume is accessible to the adsorptive species.[13]

Lowering the temperature causes the Xe resonance to shift linearly downfield, up to 144 ppm (Fig. 3), indicating increasing condensation on the micropore surface. Below 205 K an extra resonance appears, due to xenon condensation on the particles' external surfaces that competes with sorption within the micropores.[12] Thus, below 205 K the chemical shift of the confined xenon remains virtually unchanged. The easy accessibility of the galleries created by the ammonium pillars was demonstrated by the fact that the signal of the confined-xenon was recorded in less than 200 ms from when the flow of hyperpolarized Xe was put into contact with the sample. In addition, the lipophilic nature of xenon allows favourable interactions with organic TEA even in the extreme dilution of 1.25% of the gas mixture. The overall adsorption energy of xenon in the galleries amounts to 14 kJ mol^{-1}.[14]

The nanoporosity generated by pillared cations can be exploited for the adsorption of small organic molecules and gases. We tested benzene adsorption from the vapor phase at low pressure (within the ideal range), reaching an adsorption capacity of up to 50 $cm^3\ g^{-1}$ (STP) at $P/P_0 = 0.6$ and 295 K (Fig. 4). Important gases such as methane and carbon dioxide could be stored in the organoclay with remarkable efficiency. The isotherm for methane at 195 K presents a typical type I curve that at 1 atm has not yet

 This journal is © The Royal Society of Chemistry 2006

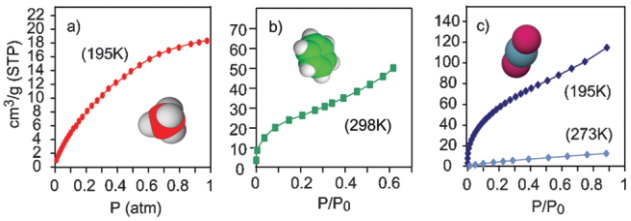

Fig. 4 Adsorption isotherms of a) methane, b) benzene and c) carbon dioxide in TEA-hectorite.

reached the saturation value. Microporous organoclay can store up to 0.63 mol of CH_4 per mol of formula unit, which represents a ratio of 1.26 with respect to the tetraethylammonium pillars. The uptake value of methane in TEA-hectorite is comparable with the values of other efficient microporous materials[6,15] and its adsorption energy is accounted for at 15 kJ mol^{-1}. A remarkable 18% of CO_2 uptake by weight is obtained at 195 K and 600 torr corresponding to 90 cm^3 g^{-1} (STP). Half of this value is already reached at 100 torr, due to the notable CO_2 adsorption energy of 26 kJ mol^{-1} in the polar environment, and corresponds to 50% filling of the interpillar spaces (3.3 moles of CO_2 per mole of TEA).[15]

In conclusion, the nanoporosity of a pillared hectorite has been described by the non conventional tool of hyperpolarized Xe NMR, demonstrating the open pore accessibility of the structure to gases. The space available for xenon diffusion was established following the 2D Lee–Goldburg MAS NMR experiments that directly detect the intercalation of bulky organic cations and their intimacy with the inorganic layers. By this innovative methodology we were able to collect, with unprecedented accuracy, the pictures of both the solid and empty parts of the porous structure at the nanometric scale. The use of spectroscopic techniques to collect, with a high level of detail, the location of pillars and the diffusion of guest species should help in the design of the structure of novel nanoporous hybrid materials for targeted applications.

This work was supported by Fondazione Cariplo and the Italian Ministry of University and Research. We are grateful to Alice Cattaneo for collaboration on the 2D NMR experiments.

Notes and references

1 R. Matsuda, R. Kitaura, S. Kitagawa, Y. Kubota, R. V. Belosludov, T. C. Kobayashi, H. Sakamoto, T. Chiba, M. Takata, Y. Kawazoe and Y. Mita, *Nature*, 2005, **436**, 238–241; S. R. Miller, P. A. Wright, C. Serre, T. Loiseau, J. Marrot and G. Férey, *Chem. Commun.*, 2005, 3850–3852; X. Zhao, B. Xiao, A. J. Fletcher, K. M. Thomas, D. Bradshaw and M. J. Rosseinsky, *Science*, 2004, **306**, 1012–1015.

2 D. W. Breck, in *Zeolite Molecular Sieves. Structure, Chemistry and Use*, Wiley, New York, 1984; A. K. Cheetham and P. M. Forster, in *Chemistry of Nanomaterials*, ed. C. N. R. Rao, A. Mueller and A. K. Cheetham, Wiley-VCH Verlag, Weinheim, 2004, vol. 2, pp. 589–619; M. W. Anderson, O. Terasaki, T. Ohsuna, A. Philippou, S. P. MacKay, A. Ferreira, J. Rocha and S. Lidin, *Nature*, 1994, **367**, 347.

3 O. M. Yaghi, M. O'Keeffe, N. W. Ockwig, H. K. Chae, M. Eddaoudi and J. Kim, *Nature*, 2003, **423**, 705–714; S. Kitagawa, R. Kitaura and S. Noro, *Angew. Chem., Int. Ed.*, 2004, **43**, 2334–2375; J. S. Seo, D. Whang, H. Lee, S. I. Jun, J. Oh, Y. J. Jeon and K. Kim, *Nature*, 2000, **404**, 982–986; L. Dobrzanska, G. O. Lloyd, H. G. Raubenheimer and L. J. Barbour, *J. Am. Chem. Soc.*, 2005, **127**, 13134–13135; E. Deiters, V. Bulach and M. W. Hosseini, *Chem. Commun.*, 2005, 3906–3908.

4 P. Sozzani, S. Bracco, A. Comotti, L. Ferretti and R. Simonutti, *Angew. Chem., Int. Ed.*, 2005, **44**, 1816–1820; N. Malek, T. Maris, M.-È. Perron and J. D. Wuest, *Angew. Chem., Int. Ed.*, 2005, **44**, 4021–4025; J. L. Atwood, L. J. Barbour, P. K. Thallapally and T. B. Wirsig, *Chem. Commun.*, 2005, 51–53; C. H. Görbitz, M. Nilsen, K. Szeto and L. W. Tangen, *Chem. Commun.*, 2005, 4288–4290.

5 T. Jiang, A. J. Lough, G. A. Ozin, D. Young and R. L. Bedard, *Chem. Mater.*, 1995, **7**, 245–248; T. J. Pinnavaia, *Science*, 1983, **220**, 365–371.

6 B. Y. Chen, H. Kim, S. D. Mahanti, T. J. Pinnavaia and Z. X. Cai, *J. Chem. Phys.*, 1994, **100**, 3872–3880; R. M. Barrer and R. J. B. Craven, *J. Chem. Soc., Faraday Trans.*, 1992, **88**, 645–651; H. Nijs, P. Cool and E. F. Vansant, *Interface Sci.*, 1997, **5**, 83–94.

7 D. Raftery, H. Long, T. Meersmann, P. J. Grandinetti, L. Reven and A. Pines, *Phys. Rev. Lett.*, 1991, **66**, 584–587; I. L. Moudrakovski, A. Nossov, S. Lang, S. R. Breeze, C. I. Ratcliffe, B. Simard, G. Santyr and J. A. Ripmeester, *Chem. Mater.*, 2000, **12**, 1181–1183; P. Sozzani, A. Comotti, R. Simonutti, R. Meersmann, J. W. Logan and A. Pines, *Angew. Chem., Int. Ed.*, 2000, **39**, 2695–2698.

8 K. A. Carrado, L. Xu, D. M. Gregory, K. Song, S. Seifert and R. E. Botto, *Chem. Mater.*, 2000, **12**, 3052; K. A. Carrado, *Appl. Clay Sci.*, 2000, **17**, 1.

9 E. Vinogradov, P. K. Madhu and S. Vega, *Chem. Phys. Lett.*, 1999, **314**, 443–450; B.-J. van Rossum, H. Förster and H. J. M. de Groot, *J. Magn. Reson.*, 1997, **124**, 516–519; S. C. Christiansen, D. Zhao, M. T. Janicke, C. C. Landry, G. D. Stucky and B. F. Chmelka, *J. Am. Chem. Soc.*, 2001, **123**, 4519–4529; S. S. Hou, F. L. Beyer and K. Schmidt-Rohr, *Solid State Nucl. Magn. Reson.*, 2002, **22**, 110–127; P. Sozzani, A. Comotti, S. Bracco and R. Simonutti, *Chem. Commun.*, 2004, 768–769.

10 By the analysis of the nitrogen isotherm at 77 K, using the Barrett–Joyner–Halenda cylindrical model, a pore diameter of 8 nm on the adsorption branch is determined and the pore volume is evaluated as 0.42 ml g^{-1}.

11 J. Demarquay and J. Fraissard, *Chem. Phys. Lett.*, 1987, **136**, 314–318.

12 P. J. Barrie, G. F. McCann, I. Gameson, T. Rayment and J. Klinowski, *J. Phys. Chem.*, 1991, **95**, 9416.

13 The total interlayer space is estimated to be 290 $Å^3$ per unit cell and the space occupied by the ammonium pillars (taking into account the stoichiometry of 0.5 and a diameter of 6 Å) is 85 $Å^3$. We can calculate the accessible space explored by in-diffusing gases to be a fraction of 0.7 (205 $Å^3$).

14 In the fast exchange regime and assuming the physiadsorption of xenon, the chemical shift dependence on temperature allows measurement of the adsorption enthalpy according to reference: I. L. Moudrakovski, V. V. Terskikh, C. I. Ratcliffe, J. Ripmeester, L.-Q. Wang, Y. Shin and G. J. Exarhos, *J. Phys. Chem. B*, 2002, **106**, 5938–5946.

15 D. N. Dybtsev, H. Chun, S. H. Yoon, D. Kim and K. Kim, *J. Am. Chem. Soc.*, 2004, **126**, 32–33; L. Pan, K. M. Adams, H. E. Hernandez, X. Wang, C. Zheng, Y. Hattori and K. Kaneko, *J. Am. Chem. Soc.*, 2003, **125**, 3062–3067; R. Choudhary and S. Mayadevi, *Zeolites*, 1996, **17**, 501–507. The isosteric enthalpies were calculated at constant surface coverage following the equation $\ln(p) = \Delta H/RT - \Delta S/R$ and by the linear fitting of the Dubinin–Radushkevich plot taking into account the vaporization enthalpies of the two gases: F. Rouquerol, J. Rouquerol and K. Sing, in *Adsorption by Powders and Porous Solids*, Academic Press, London, 1999.